Available online at www.sciencedirect.com
SCIENCE DIRECT®
Journal of Molecular Spectroscopy 228 (2004) 110–119
Journal of MOLECULAR SPECTROSCOPY
www.elsevier.com/locate/jms

High-resolution Fourier transform spectrum of H_2S in the region of 8500–8900 cm^{-1}

O.N. Ulenikov[a,b], A.-W. Liu[a], E.S. Bekhtereva[a,b], S.V. Grebneva[b], W.-P. Deng[a], O.V. Gromova[b], S.-M. Hu[a,*]

[a] *Laboratory of Bond Selective Chemistry, University of Science and Technology of China, Hefei 230026, China*
[b] *Laboratory of Molecular Spectroscopy, Department of Physics, Tomsk State University, Tomsk 634050, Russia*

Received 30 March 2004; in revised form 16 July 2004
Available online 20 August 2004

Abstract

High-resolution Fourier transform infrared spectrum of H_2S was recorded and analyzed in the region of the $v = v_1 + \frac{1}{2}v_2 + v_3 = 3.5$ polyad. More than 450 transitions were assigned to the $3v_1 + v_2$ and $2v_1 + v_2 + v_3$ bands with the maximum values of quantum numbers J and K_a equal to 14, 7, and 14, 9 for these two bands, respectively. The theoretical analysis was fulfilled with the Hamiltonian which takes into account strong resonance interactions among the studied vibrational states (3 1 0), (2 1 1), and also "dark" states (0 3 2) and (2 3 0). The *rms* deviation is 0.0019 cm^{-1}. The intensity borrowing effect in the doublets in the P-branch transitions of the $3v_1 + v_2$ and $2v_1 + v_2 + v_3$ bands is observed and discussed.

Keywords: Vibration–rotation spectra; H_2S molecule; Resonance interactions; Spectroscopic parameters

1. Introduction

In a recent contribution [1], we presented results of analysis of the high-resolution Fourier transform spectrum of the H_2S molecule in the region of the $v = v_1 + \frac{1}{2}v_2 + v_3 = 3$ polyad (7300–7900 cm^{-1}). The goal of the present investigation is the high-resolution analysis of the H_2S spectrum in the shorter wave region, namely, 8500–8900 cm^{-1}, where the next, $v = 3.5$ polyad is located.

Because the review of the earlier investigations of the H_2S spectra was made in [1], we will not repeat it here. As to the high-resolution spectrum in the region discussed in the present study, it was mentioned in [2] and only a few information was reported: the numbers of assigned transitions (74 and 86), maximum values of the upper quantum numbers J and K_a ($J = 9$, $K_a = 7$ and $J = 9$, $K_a = 8$), and values of the band centers (8697.142 and 8697.155 cm^{-1}) for the parallel and perpendicular type bands, $3v_1 + v_2$ and $2v_1 + v_2 + v_3$, respectively.

In the present study, we report the results of the experimental recording and theoretical analysis which allowed us to assign more than 450 transitions with the maximum values of the upper quantum numbers J and K_a equal 14, 7 and 14, 9 for the parallel and perpendicular bands, respectively. Section 2 presents the experimental details. Hamiltonian used for analysis of experimental data is given in Section 3. Description of the spectrum and assignments of the recorded transitions are presented in Section 4. Results of the fit and discussions can be found in Section 5.

2. Experimental details

The H_2S sample was purchased from Nanjing Special Gas Company with a stated purity of 99%. The high-resolution spectra of H_2S in the 8500–8900 cm^{-1} region

* Corresponding author. Fax: +86 551 360 2969.
E-mail addresses: Ulenikov@phys.tsu.ru (O.N. Ulenikov), smhu@ustc.edu.cn (S.-M. Hu).

0022-2852/$ - see front matter © 2004 Elsevier Inc. All rights reserved.
doi:10.1016/j.jms.2004.07.011

were recorded with a Bruker IFS 120 HR Fourier transform spectrometer (Hefei, China) equipped with a path length adjustable multi-pass gas cell at room temperature. A tungsten source, a Ge detector, and a CaF_2 beam-splitter were used. The unapodized spectral resolution was 0.015 cm^{-1}. The absorption path length was 105 m, and the pressure was 2076 Pa. An overview of the spectrum is presented in Fig. 1. The line positions were calibrated using H_2O lines listed in HITRAN-96 database. The accuracy of line positions of unblended and not-very-weak lines was estimated to be 0.002–0.003 cm^{-1} or better.

3. Theoretical background

The H_2S molecule is an asymmetric top of the C_{2v} symmetry with the value of the asymmetry parameter $\kappa \simeq 0.532$. Its three fundamental bands v_1, v_2, and v_3 are located at 2614.44, 1182.53, 2628.37 cm^{-1} and have the symmetries A_1, A_1, and B_2, respectively. As a consequence,

(a) the selection rules of the ro-vibrational transitions of H_2S are:

$$\Delta J = 0, \pm 1; \quad \Delta K_a = \pm(2n+1); \quad \Delta K_c = \pm(2m+1) \tag{1}$$

for the bands with v_3 even, and

$$\Delta J = 0, \pm 1; \quad \Delta K_a = \pm 2n; \quad \Delta K_c = \pm(2m+1) \tag{2}$$

for the bands with v_3 odd. Here $n,m = 0,1,2,\ldots$ When $n = m = 0$, transitions are called as "allowed," otherwise, transitions are called as "forbidden";

(b) the so-called polyad of interacting vibrational states is consisted of the vibrational states with a fixed value of quantum number v ($v = v_1 + \frac{1}{2}v_2 + v_3$). In this case, states within a polyad can strongly perturb each other by Fermi and/or Coriolis-type interactions.

Taking into account all the above said, the Hamiltonian for the $v = v_1 + \frac{1}{2}v_2 + v_3 = 3.5$ polyad should be used in the following form:

$$H^{\text{v.-r.}} = \sum_{v,v'} H^{vv'} |v\rangle\langle v'|, \tag{3}$$

where 10 vibrational states in this $v = 3.5$ polyad should be included in the summation: $(3\,1\,0, A_1)$, $(2\,1\,1, B_2)$, $(1\,1\,2, A_1)$, $(0\,1\,3, B_2)$, $(2\,3\,0, A_1)$, $(1\,3\,1, B_2)$, $(0\,3\,2, A_1)$, $(1\,5\,0, A_1)$, $(0\,5\,1, B_2)$, and $(0\,7\,0, A_1)$. However, since all the bands are weak, and only two strongest bands appear in the recorded spectrum, we reduced the number of states in the Hamiltonian (3) to two at the beginning, they are $(3\,1\,0, A_1)$ and $(2\,1\,1, B_2)$ ($(30^+, 1)$ and $(30^-, 1)$ states in the local mode notations). Then, as the further analysis shows, to reach a correct description of the recorded transitions, we must take into account the interactions not only between the "bright" states $(3\,1\,0, A_1)$ and $(2\,1\,1, B_2)$, but also among the "dark" states, $(1\,1\,2, A_1)$ and

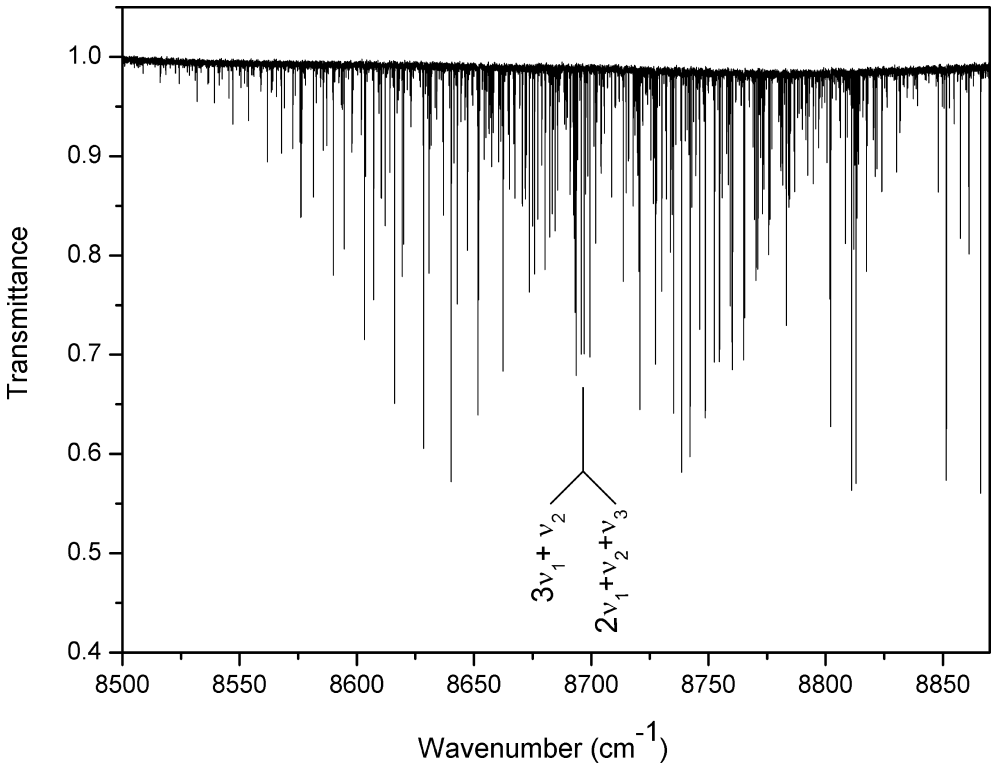

Fig. 1. Survey spectrum of H_2S molecule in the region of 8500–8900 cm^{-1}. Centers of the bands $3v_1 + v_2$ and $2v_1 + v_2 + v_3$ located in this region are denoted. Strong lines belonging to the water vapor can be seen at the right-hand side of the figure. Experimental conditions: absorption path length, 105 m; sample pressure, 2076 Pa; instrumental resolution, 0.015 cm^{-1}; room temperature.

$(0\,1\,3, B_2)$ in the higher energy region, and at least, $(2\,3\,0, A_1)$ and $(0\,3\,2, A_1)$ in the lower energy region. So, finally, six vibrational states were used in the Hamiltonian (3) with the notations: $|1\rangle = (3\,1\,0, A_1)$, $|2\rangle = (0\,3\,2,\ A_1)$, $|3\rangle = (2\,3\,0, A_1)$, $|4\rangle = (1\,1\,2, A_1)$, $|5\rangle = (0\,1\,3, B_2)$, and $|6\rangle = (2\,1\,1, B_2)$.

The diagonal blocks H^{vv} in Eq. (3) have the form of usual Watson-type operators, [3], and they describe rotational structures of corresponding vibrational states:

$$\begin{aligned} H^{vv} = {} & E^v + \left[A^v - \frac{1}{2}(B^v + C^v)\right] J_z^2 + \frac{1}{2}(B^v + C^v) J^2 \\ & + \frac{1}{2}(B^v - C^v) J_{xy}^2 - \Delta_K^v J_z^4 - \Delta_{JK}^v J_z^2 J^2 - \Delta_J^v J^4 \\ & - \delta_K^v [J_z^2, J_{xy}^2] - 2\delta_J^v J^2 J_{xy}^2 + H_K^v J_z^6 + H_{KJ}^v J_z^4 J^2 \\ & + H_{JK}^v J_z^2 J^4 + H_J^v J^6 + [J_{xy}^2, h_K^v J_z^4 + h_{JK}^v J^2 J_z^2 + h_J^v J^4] \\ & + L_K^v J_z^8 + L_{KKJ}^v J_z^6 J^2 + L_{JK}^v J_z^4 J^4 + L_{KJJ}^v J_z^2 J^6 + L_J^v J^8 \\ & + [J_{xy}^2, l_K^v J_z^6 + l_{KJ}^v J^2 J_z^4 + l_{JK}^v J^4 J_z^2 + l_J^v J^6] \\ & + P_K^v J_z^{10} + [J_{xy}^2, p_K^v J_z^8] + \cdots \end{aligned} \tag{4}$$

Non-diagonal operators $H^{vv'}$, $(v \neq v')$, describe resonance interactions between the states $|v\rangle$ and $|v'\rangle$. In this case, resonance interactions between the states of the same symmetry, either A_1 or B_2, are described by the Fermi-type operators:

$$\begin{aligned} H_F^{vv'} = {} & F^{vv'} + F_K^{vv'} J_z^2 + \cdots + F_{xy}^{vv'} J_{xy}^2 + F_{xyK}^{vv'} [J_{xy}^2, J_z^2]_+ \\ & + F_{xyJ}^{vv'} J_{xy}^2 J^2 + \cdots \end{aligned} \tag{5}$$

where it is denoted $J_{xy}^2 = J_x^2 - J_y^2$ and $J^2 = J_x^2 + J_y^2 + J_z^2$. Coriolis-type non-diagonal operators $H^{vv'}$ describe resonance interactions between the states $|v\rangle$ and $|v'\rangle$ of different symmetries, with one A_1 and another one B_2:

$$\begin{aligned} H_{Cy}^{vv'} = {} & 2(B\zeta^y)^{vv'} i J_y + C_{yK}^{vv'} [i J_y, J_z^2]_+ + C_{yJ}^{vv'} i J_y J^2 \\ & + C_{yKK}^{vv'} [i J_y, J_z^4]_+ + C_{yJK}^{vv'} [i J_y, J_z^2 J^2]_+ \\ & + C_{yJJ}^{vv'} i J_y J^4 + \cdots + C_{xz}^{vv'} [J_x, J_z]_+ \\ & + C_{xzK}^{vv'} [[J_x, J_z]_+, J_z^2]_+ + C_{xzJ}^{vv'} [J_x, J_z]_+ J^2 + \cdots \\ & + C_{yxy}^{vv'} [i J_y, J_{xy}^2]_+ \cdots \end{aligned} \tag{6}$$

For the convenience of the reader, diagram in Eq. (7) clarifies the structure of the matrix of effective Hamiltonian (3):

$$H^{vv'} = \begin{vmatrix} (310) & (032) & (230) & (112) & (013) & (211) \\ W & - & F & D & - & C \\ - & W & D & F & C & - \\ F & D & W & - & - & C \\ D & F & - & W & C & C \\ - & C & - & C & W & D \\ C & - & C & C & D & W \end{vmatrix}. \tag{7}$$

4. Description of the spectrum and assignment of transitions

The survey spectrum of H_2S molecule in the region of 8500–8900 cm^{-1} is shown on Fig. 1. On that figure, one can easily recognize typical structures of the Q-branch near the 8697 cm^{-1}, and of the P- and R-branches. A set of strong lines in the shorter wavelength region of the figure belongs to the H_2O molecule. As it can be expected, the P-branch is about two times broader than the R-branch. No other weak bands can be recognized in the survey spectrum.

Assignments of transitions were made with the traditional Ground State Combination Differences method. The ground state energies were calculated on the base of parameters from [4]. More than 450 transitions with $J^{max} = 14$ and 14, $K_a^{max} = 7$ and 9 were assigned to the bands $3\nu_1 + \nu_2$ and $2\nu_1 + \nu_2 + \nu_3$, respectively. For illustration, two small parts of the recorded spectrum with the assignments of transitions are shown on Figs. 2 and 3. Thereof 101 ro-vibrational energies of the state (3 1 0) and 95 of the (2 1 1) state were obtained, which are given in Table 1 together with their experimental uncertainties Δ. Since the upper ro-vibrational energies were determined from several transitions reaching the same upper level, their uncertainties Δ can be considered as an indication of the precision of the experimental line positions. Thus the average experimental accuracy of the line positions can be estimated as 0.002–0.003 cm^{-1} for unblended and not-very-weak lines. With increasing value of the quantum number J, the accuracy of line positions decrease because of the decreasing in line strengths.

As the result, practically all the recorded experimental transitions in the region of 8500–8870 cm^{-1} were assigned to the $3\nu_1 + \nu_2$ and $2\nu_1 + \nu_2 + \nu_3$ bands. This fact confirms the statement about the weakness of the other bands in this polyad $(\nu_1 + \frac{1}{2}\nu_2 + \nu_3 = 3\frac{1}{2})$.

5. Results and discussion

As was mentioned above, there are some other vibrational states (see Table 2 which is reproduced from Table IV in [5]) which may perturb the ro-vibrational structures of the studied states (3 1 0) and (2 1 1). They are, first of all, the states (1 1 2) and (0 1 3) which strongly perturb the states (3 1 0) and (2 1 1), respectively, by the Darling–Dennison interaction. The state (0 8 0) does not exert influence on the studied states. Other vibrational states in the shorter wave region are very far from the states of interest here. While as the analysis shows, according to our experimental data, the influence from the states (0 3 2) and (2 3 0) located in the longer wave region is important for the local perturbations in the ro-vibrational structures of the states (3 1 0) and (2 1 1). For

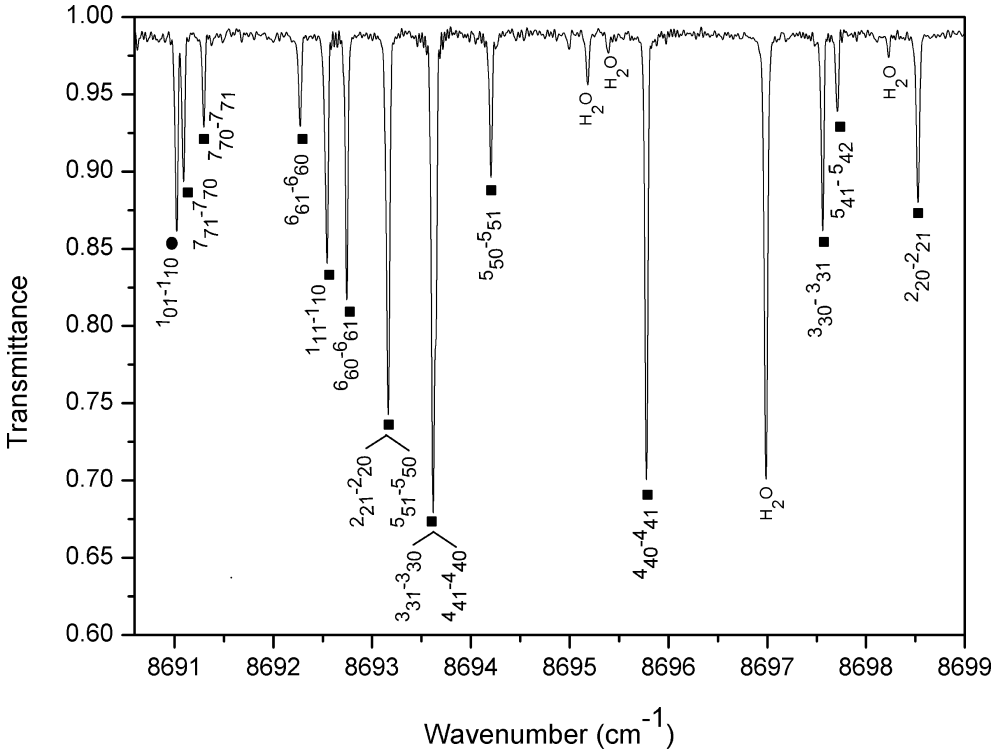

Fig. 2. Small portion of the Q-branch of $3\nu_1 + \nu_2$ (marked by dark circle) and $2\nu_1 + \nu_2 + \nu_3$ (dark squares). Experimental conditions: absorption path length, 105 m; sample pressure, 2076 Pa; instrumental resolution, 0.015 cm^{-1}; room temperature.

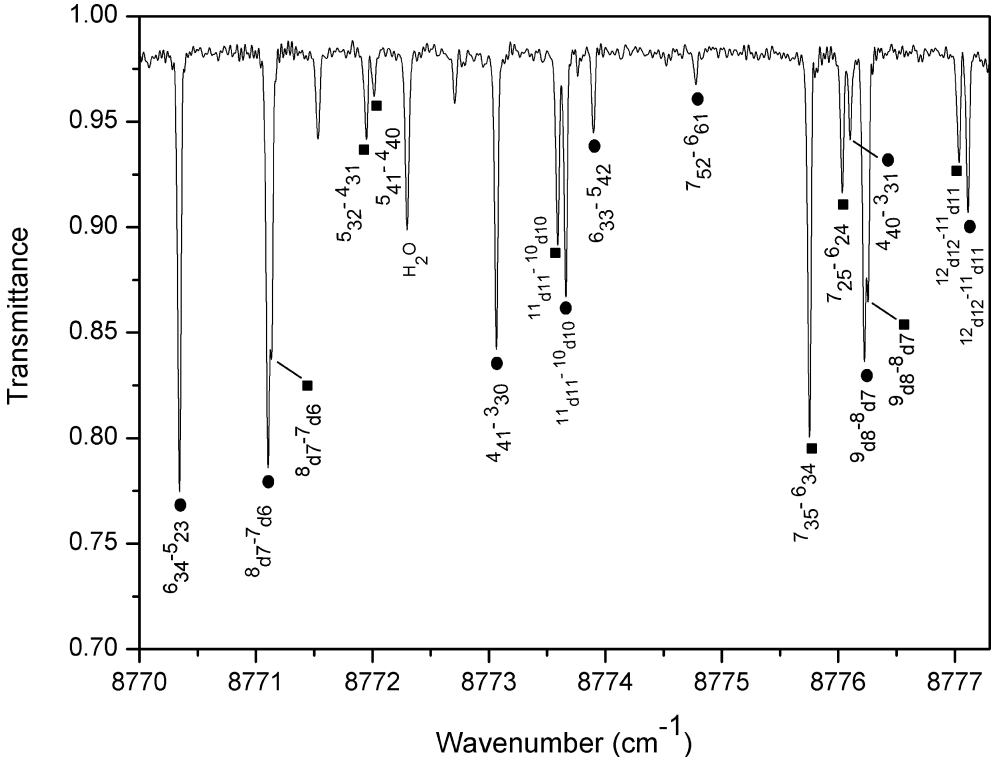

Fig. 3. Small part of the R-branches of $3\nu_1 + \nu_2$ (marked by dark circle) and $2\nu_1 + \nu_2 + \nu_3$ (dark squares). Experimental conditions: absorption path length, 105 m; sample pressure, 2076 Pa; instrumental resolution, 0.015 cm^{-1}; room temperature.

Table 1
Experimental ro-vibrational energy levels for the (310) and (211) vibrational states of the H_2S molecule (cm^{-1})

J	K_a	K_c	(310)			(211)		
			E	Δ[a]	δ[b]	E	Δ[a]	δ[b]
	1		2	3	4	5	6	7
0	0	0				8697.1570		−7
1	0	1	8710.3982		16	8710.4130	17	15
1	1	1	8711.9078	10	16	8711.9195	1	3
1	1	0	8716.2019	3	15	8716.2133	11	−14
2	0	2	8733.7793	2	−9	8733.7919	5	10
2	1	2	8734.1184	6	7	8734.1275	12	−6
2	1	1	8746.9867		−7	8747.0014	2	−7
2	2	1	8751.5068	11	2	8751.5146		−7
2	2	0	8754.6197		15	8754.6276	3	−16
3	0	3	8765.7894	6	−28	8765.7998		25
3	1	3	8765.8440	7	4	8765.8506	15	17
3	1	2	8789.6515	4	0	8789.6635	17	5
3	2	2	8791.2368	7	−11	8791.2477	8	−1
3	2	1	8802.0476		30	8802.0598	8	3
3	3	1	8811.0050	23	4	8811.0079	10	8
3	3	0	8812.8988	15	13	8812.9014	6	−12
4	0	4	8806.6203	11	20	8806.6330	35	−20
4	1	4				8806.6380		24
4	1	3	8841.0674	13	−23	8841.0777	12	6
4	2	3	8841.4087	11	−12	8841.4185	6	0
4	2	2	8863.2732	10	1	8863.2884	13	4
4	3	2	8867.5255	15	10	8867.5324	12	−14
4	3	1	8875.8369	8	−17	8875.8520	8	−18
4	4	1	8890.4566	5	−1	8890.4510	29	6
4	4	0	8891.4443	20	−4	8891.4385	4	−18
5	0	5	8856.3750	110	−101	8856.3750	110	110
5	1	5	8856.3750	110	−107	8856.3750	110	114
5	1	4	8900.9175	12	−14	8900.9197		−36
5	2	4	8900.9772	11	−4	8900.9839	3	26
5	2	3	8934.3353	14	11	8934.3467	4	−2
5	3	3	8935.6051	7	−14	8935.6214	6	35
5	3	2	8954.5786	7	22	8954.5968	9	9
5	4	2	8963.0702	7	−8	8963.0816	11	20
5	4	1	8968.8032	7	2	8968.8159	9	−13
5	5	1	8989.8648	4	3	8989.8462		7
5	5	0	8990.3268	2	4	8990.3096	16	10
6	0	6	8915.0702	4	26	8915.0410	18	13
6	1	6	8915.0702	4	25	8915.0410	18	14
6	1	5	8969.5629	16	37	8969.5449	37	−28
6	2	5	8969.5629	16	50	8969.5449	37	−36
6	2	4	9013.4092	22	5	9013.4210	8	8
6	3	4	9013.6877	10	17	9013.6975		0
6	3	3	9045.0032	10	−27	9045.0266	6	−5
6	4	3	9048.4077	15	6	9048.3790	12	0
6	4	2	9063.7921		−30	9063.8217	3	18
6	5	2	9077.9615	16	−16	9077.8790	6	−3
6	5	1	9081.4560		3	9081.5239	10	−3
6	6	1	9109.1561	22	−1	9109.1200	14	14
6	6	0	9109.3570		−4	9109.3201	9	−3
7	0	7	8982.6764	12	18	8982.6415	6	−15
7	1	7	8982.6764	12	17	8982.6415	6	−15
7	1	6	9047.0578	130	38	9047.0578	130	−23
7	2	6	9047.0578	130	38	9047.0578	130	−7
7	2	5	9100.8998	23	10			
7	3	5	9100.9535	20	73			
7	3	4	9143.6362	3	−23			
7	4	4	9144.5841	11	7	9144.5972	6	−41
7	4	3	9172.6835	14	−14	9172.7183	11	−22
7	5	3	9179.8440	11	4	9179.8357	4	20
7	5	2	9191.3509	19	35			

Table 1 (*continued*)

J	K_a	K_c	(310)			(211)		
			E	Δ[a]	δ[b]	E	Δ[a]	δ[b]
	1		2	3	4	5	6	7
7	6	2	9212.2438		−55	9212.2059	17	2
7	6	1	9214.1399	12	−57	9214.1000	43	−69
7	7	1	9248.1890		−30	9248.1220	4	−7
7	7	0	9248.2741	19	9	9248.2039		−22
8	0	8	9059.1918	13	−27	9059.1378	98	−53
8	1	8	9059.1918	13	−27	9059.1378	98	−53
8	1	7	9133.4825	30	3	9133.4542	42	33
8	2	7	9133.4825	30	−17	9133.4542	42	37
8	2	6	9197.1236		−43			
8	3	6	9197.1264		41			
8	3	5	9250.0787		97	9250.1002	2	60
8	4	5	9250.3014	18	30			
8	4	4	9290.9860	13	−2	9291.0305	13	14
8	5	4	9293.5500	16	−63			
8	5	3	9317.3752		−50	9317.6327	5	−1
8	6	3	9329.9852	4	7			
8	6	2	9337.7877		90	9337.7561	15	−35
8	7	2	9365.9140	11	12			
8	7	1				9366.7800	48	0
8	8	0				9406.6923	8	11
9	0	9	9144.6210	8	0	9144.5722	2	5
9	1	9	9144.6210	8	0	9144.5722	2	5
9	1	8	9228.7498	10	0	9228.7184	4	−17
9	2	8	9228.7498	10	0	9228.7184	4	−17
9	2	7	9302.0710	12	15			
9	3	7	9302.0710	12	−10			
9	4	6	9364.9583		−53			
9	9	1				9584.5073		0
10	0	10	9238.9389	2	10	9238.8804		−5
10	1	10	9238.9389	2	10	9238.8804		−5
10	1	9	9332.9189	7	−9	9332.8809		17
10	2	9	9332.9189	7	−9	9332.8809		17
10	2	8				9416.0180	23	−13
10	3	8				9416.0180	23	−9
11	0	11	9342.1296	38	−17	9342.0637		−6
11	1	11	9342.1296	38	−17	9342.0637		−6
11	1	10	9445.9472	9	−3	9445.9021		12
11	2	10	9445.9472	9	−3	9445.9021		12
11	2	9				9538.6735	15	2
11	3	9				9538.6735	15	3
12	0	12	9454.1865	13	16	9454.1087		18
12	1	12	9454.1865	13	16	9454.1087		18
12	1	11	9567.8205	6	3	9567.7683		−13
12	2	11	9567.8205	6	3	9567.7683		−13
13	0	13	9575.0811	2	0	9574.9902		−8
13	1	13	9575.0811	2	0	9574.9902		−8
13	1	12	9698.5451		79			
13	2	12	9698.5451		79			
14	0	14	9704.8036	6	−3	9704.6950		0
14	1	14	9704.8036	6	−3	9704.6950		0

[a] Δ is the experimental uncertainty (1σ) of the energy value, in 10^{-4} cm^{-1}; Δ is not quoted when the energy value was obtained from only one transition.

[b] $\delta = E^{\text{exp.}} - E^{\text{calc.}}$, in 10^{-4} cm^{-1}.

an illustration, Fig. 4 shows an example of such kind of perturbations. The plots Ia and IIa give the values of the difference $\delta_E = E^{\text{exp.}} - E^{\text{calc.}}$ versus the quantum number J for the $[J, K_a = J - 1, K_c = 1]$ (2 1 1) and $[J, K_a = J - 1,\ K_c = 2]$ (2 1 1) levels, respectively. Here $E^{\text{calc.}}$ is calculated without the resonance interaction between the (2 1 1) and other vibrational states taken into account. One can see typical appearance of resonance interaction at $J = 6$. As the analysis shows, there is a resonance with the closely located ro-vibrational energy

Table 2
Some calculated vibrational levels of the H_2S molecule (cm^{-1})

v_1	v_2	v_3	E_{vib}
1	5	0	8317.74
1	3	1	8538.93
2	3	0	8539.53
0	3	2	8637.92
2	1	1	8696.48
3	1	0	8696.58
1	1	2	8877.73
0	1	3	8898.66
0	8	0	9095.86
0	6	1	9411.66

levels $[J = 6\ K_a = 6\ K_c = d]$ $(d = 0, 1)$ of the (0 3 2) vibrational state. And, in this case, the energy value of the level [6 5 2](2 1 1) is less than that of [6 6 0](2 3 0). On the contrary, the value $E_{[6\,5\,1](2\,1\,1)}$ is larger than that of $E_{[6\,6\,1](2\,3\,0)}$. This circumstance clearly explains the behavior of the Ia and IIa curves. The plots Ib and IIb illustrate the behavior of the δ_E values when the resonance interaction with the (2 3 0) state was taken into account. One can see good correspondence between experimental and calculated values in that case.

One more interesting effect should be discussed here, which is illustrated by Fig. 5. On the top line of that figure, one can clearly see sets of doublets $[J + 1\ d\ J + 1] \leftarrow [J\ d\ J]$ $(d = 0, 1)$ which belong to the $3v_1 + v_2$ and $2v_1 + v_2 + v_3$ bands, respectively. It is important that in most cases, the distances between the components of doublets are considerably larger than the spectral resolution in our experiment. At the same time, in the *P*-branch, which fragments are shown on the bottom line of Fig. 5, there is no doublet evidenced, but single lines can be seen for most of the $[J - 1\ d\ J - 1] \leftarrow [J\ d\ J]$ transitions. The reason of the effect is in the near local mode nature of the considered states $(3\,0^+, 1)$ and $(3\,0^-, 1)$, which are the mixtures of the states (3 1 0)/(1 1 2) and (2 1 1)/(0 1 3) in the normal mode notations, respectively. In addition, if one will take into account the presence of strong Coriolis interaction between the states $(3,0^+, 1)$ and $(3\,0^-, 1)$, the intensity borrowing effect by one of the components $[J - 1\ dJ{-}1] \leftarrow [J\ d\ J]$ in the *P*-branch can be explained on the basis of analysis of dipole moment matrix elements [6].

As was discussed above, the Hamiltonian (3)–(6) was used for the fit of the experimental upper energies listed in Table 1. The initial values of the effective Hamiltonian parameters were selected in the following way:

(1) The initial values of the band centers were taken from Table IV of [5], and the values of resonance interaction parameters $F^{3\,1\,0\text{–}1\,1\,2}$ and $F^{0\,1\,3\text{–}2\,1\,1}$ were estimated on the base of $\Gamma_{D.-D.}$ constant from [2]. In this case, the vibrational energies $E_{(1\,1\,2)}$ and $E_{(0\,1\,3)}$ were constrained to the values 8828.08 and

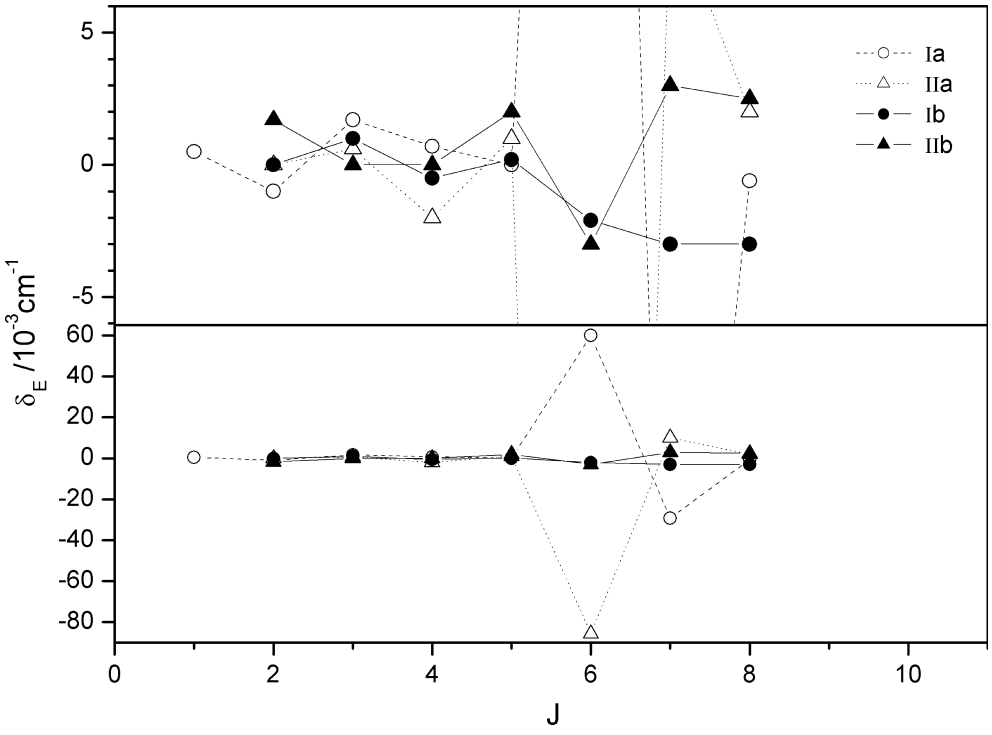

Fig. 4. The illustration of the strong local resonance interaction between the (2 1 1) and (0 3 2) vibrational states. The plots I and II give the values of the difference $\delta_E = E^{exp.} - E^{calc.}$ versus the value of quantum number *J* for the $[J, K_a = J - 1, K_c = 1]$ (2 1 1) and $[J, K_a = J - 1, K_c = 2]$ (2 1 1) levels, respectively. *b* and *a* note for that $E^{calc.}$ is calculated with or without the resonance interaction between the (2 1 1) and (0 3 2). The upper panel is an enlarged view of the lower panel.

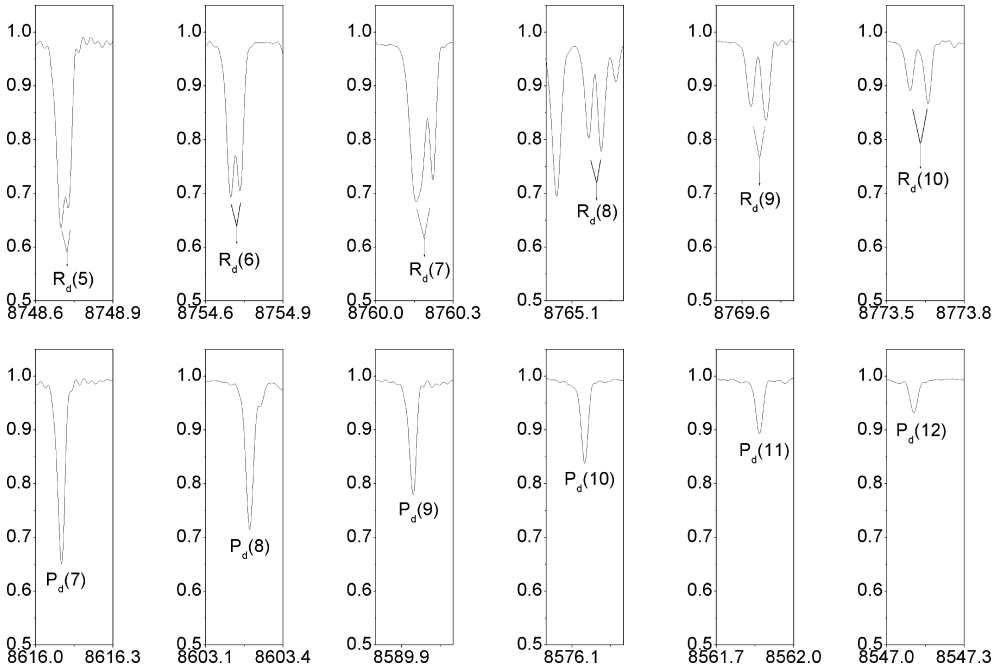

Fig. 5. Small parts of the high-resolution spectrum of H_2S illustrated the total borrowing of intensities in the $P_d(J) = [J-1\ K_a = d'\ K_c = J-1] \leftarrow [J\ K_a = d\ K_c = J]$, $(d,d' = 0$, and/or 1), doublets of the P-branch. On the top line of the figure, the doublets are clearly seen, which one components belong to the $R_d(J) = [J+1\ K_a = d'\ K_c = J+1] \leftarrow [J\ K_a = d\ K_c = J]$, $(d,d'=0$, and/or 1), transitions of the $3\nu_1 + \nu_2$ band, and another $R_d(J)$ components belong to the $2\nu_1 + \nu_2 + \nu_3$ band. At the same time, only one components are seen in the P-branch on the bottom line.

8858.32 cm^{-1}, respectively. This just correspond the band center values, 8877.73 and 8898.66 cm^{-1}, respectively, from [5].

(2) Centrifugal distortion parameters for the states (3 1 0), (2 1 1), (1 1 2), and (0 1 3) were constrained to the values of corresponding parameters of the (0 1 0) vibrational state from [7]. To estimate the values of the rotational parameters of the (1 1 2) and (0 1 3) state, we first made a testing fit of the energy values of the states (3 1 0) and (2 1 1) with $J \leqslant 2$. The mean values of the A, B, and C parameters, obtained from the testing fit, were then fixed as the A, B, and C parameters of the states (1 1 2) and (0 1 3).

(3) The initial values of centrifugal distortion parameters of the two "dark" states, (0 3 2) and (2 3 0), were constrained to the values of corresponding parameters of the (0 3 0) vibrational state from [8]. As to the initial values of rotational A, B, and C parameters, they have been extrapolated from the values of corresponding parameters of the states (0 1 0), (1 1 0), and (0 1 1) [7], and (0 3 0) [8].

(4) The initial values of all Coriolis-type interaction parameters have been set as zero.

Upper ro-vibrational energy levels from columns 2 and 5 of Table 1 were used as the input data in the fit procedure with the Hamiltonian, Eqs. (3)–(6). All the input energy levels were taken with weights proportional to $(1/\Delta^2)$, where Δ is the experimental uncertainty of corresponding energy value also presented in Table 1 (columns 3 and 6). In this case, the upper levels which are obtained from only one transition (the weights are zero), were excluded from the fit.

As the result of the fit, 46 parameters was derived (28 parameters of diagonal blocks and 18 resonance interaction parameters) which reproduce the initial upper energy levels used in the fit, with the *rms* deviation of 0.0019 cm^{-1}. The obtained parameters are presented in columns 3–8 of Table 3 and in Table 4 together with their 1σ statistical confidence intervals. Parameters presented in Table 3 without confidence intervals were constrained to their initial values as discussed above. Column 2 of Table 3, for a convenient comparison, shows the spectroscopic parameters of the ground vibrational state, which are reproduced from [4]. One can see satisfactory correlations of the parameters both between the states (3 1 0) and (2 1 1) (with the exception of parameters H_{KJ} and H_{JK}), and with the corresponding parameters of the ground vibrational state. Small discrepancies between the values of parameters H_{KJ} and H_{JK}, may be, due to the absence of some additional resonance interactions between states (3 1 0) and (2 1 1), and/or other states of this polyad. Nevertheless, the calculated energy levels reproduce the experimental values almost within the experimental uncertainties. This is illustrated by the data of columns 4 and 7 of Table 1 where the values of $\delta = E^{\text{exp.}} - E^{\text{calc.}}$ are given for upper energies.

Table 3
Spectroscopic parameters of some vibrational states of the H_2S molecule (cm^{-1})[a]

Parameter	(000)[b]	(310)	(211)	(112)	(013)	(032)	(230)
1	2	3	4	5	6	7	8
E	—	8746.7927(12)	8737.49720(96)	8828.08[d]	8858.32[d]	8629.940(89)	8535.03(95)
A	10.3601594	10.26055(130)	10.25636(121)	10.24[e]	10.24[e]	11.2947(168)	11.3093(586)
B	9.0181358	8.84853(130)	8.74552(226)	8.83[e]	8.83[e]	9.57883(255)	9.5247(137)
C	4.7307832	4.4311870(860)	4.53428(218)	4.48[e]	4.48[e]	4.41[f]	4.45[f]
Δ_K ($\times 10^3$)	3.70326	3.7138(171)	3.8895(191)	4.5579033[c]	4.5579033[c]	6.94186[g]	6.94186[g]
Δ_{JK} ($\times 10^3$)	−2.28026	−2.1355(173)	−2.2608(205)	−2.7348452[c]	−2.7348452[c]	−3.97768[g]	−3.97768[g]
Δ_J ($\times 10^3$)	0.652598	0.67047(528)	0.64073(482)	0.75614258[c]	0.75614258[c]	1.037139[g]	1.037139[g]
δ_K ($\times 10^3$)	−0.132618	−0.019544[c]	−0.0195444[c]	−0.0195444[c]	−0.0195444[c]	0.323995[g]	0.323995[g]
δ_J ($\times 10^3$)	0.295517	0.30189(269)	0.30455(235)	0.3473094[c]	0.3473094[c]	0.486891[g]	0.486891[g]
H_K ($\times 10^6$)	1.3811	2.6294[c]	2.6294[c]	2.6294[c]	2.6294[c]	8.022[g]	8.022[g]
H_{KJ} ($\times 10^6$)	1.2592	1.331(252)	2.903(173)	0.99673[c]	0.99673[c]	−0.7639[g]	−0.7639[g]
H_{JK} ($\times 10^6$)	−1.5329	−0.9757(728)	−2.620(166)	−1.85007[c]	−1.85007[c]	−2.9783[g]	−2.9783[g]
H_J ($\times 10^6$)	0.27098	0.39253(458)	0.36015(123)	0.374766[c]	0.374766[c]	0.71176[g]	0.71176[g]
h_K ($\times 10^6$)	1.229	2.12233[c]	2.12233[c]	2.12233[c]	2.12233[c]	5.1642[g]	5.1642[g]
h_{JK} ($\times 10^6$)	−0.48509	−0.62452[c]	−0.62452[c]	−0.62452[c]	−0.62452[c]	−1.1669[g]	−1.1669[g]
h_J ($\times 10^6$)	0.13541	0.186968[c]	0.186968[c]	0.186968[c]	0.186968[c]	0.35503[g]	0.35503[g]
L_K ($\times 10^9$)	−4.4878	−9.9918[c]	−9.9918[c]	−9.9918[c]	−9.9918[c]	−29.45[g]	−29.45[g]
L_{KKJ} ($\times 10^9$)	5.48	12.641[c]	12.641[c]	12.641[c]	12.641[c]	27.259[g]	27.259[g]
L_{KJ} ($\times 10^9$)	−3.319	−6.4092[c]	−6.4092[c]	−6.4092[c]	−6.4092[c]	−7.5[g]	−7.5[g]
L_{KJJ} ($\times 10^9$)	1.1843	1.4788[c]	1.4788[c]	1.4788[c]	1.4788[c]	2.582[g]	2.582[g]
L_J ($\times 10^9$)	−0.1395	−0.21671[c]	−0.21671[c]	−0.21671[c]	−0.21671[c]	−0.45511[g]	−0.45511[g]
l_K ($\times 10^9$)	−1.757	−4.3308[c]	−4.3308[c]	−4.3308[c]	−4.3308[c]	−10.851[g]	−10.851[g]
l_{KJ} ($\times 10^9$)	−0.301	−0.5267[c]	−0.5267[c]	−0.5267[c]	−0.5267[c]	2.555[g]	2.555[g]
l_{JK} ($\times 10^9$)	0.4051	0.47523[c]	0.47523[c]	0.47523[c]	0.47523[c]	0.7[g]	0.7[g]
l_J ($\times 10^9$)	−0.07044	−0.10858[c]	−0.10858[c]	−0.10858[c]	−0.10858[c]	−0.23[g]	−0.23[g]
P_K ($\times 10^{12}$)	3.67	16.806[c]	16.806[c]	16.806[c]	16.806[c]		
p_K ($\times 10^{12}$)	4.01	11.616[c]	11.616[c]	11.616[c]	11.616[c]		

[a] Values in parentheses are the 1σ statistical confidence intervals. Values of parameters presented in columns 3–8 without confidence intervals were fixed in the fit (see text, for details).
[b] Reproduced from [4].
[c] Constrained to the value of corresponding parameter of the (010) vibrational state [7].
[d] Constrained to the values which correspond to the centers of the bands (112) and (013), 8877.73 and 8898.66 cm^{-1}, respectively, from [5].
[e] Constrained to the mean value of corresponding parameters of the (310) and (211) states which have been estimated from the approximate ($J \leqslant 2$) fit of the states (310) and (211), see text, for details.
[f] Extrapolated from the values of corresponding parameters of the states (010), (110), and (011) [7], and (030) [8].
[g] Constrained to the value of corresponding parameter of the (030) vibrational state [8].

Table 4
Parameters of resonance interactions between the states of the ($v = 3.5$) polyad of the H_2S molecule (cm^{-1})[a]

Parameter	Value	Parameter	Value	Parameter	Value
Fermi-type interaction					
$F^{310-112}$	80.63[b]	$F_{xy}^{310-112}$ ($\times 10^2$)	4.082(391)		
$F^{013-211}$	80.63[b]	$F_{xy}^{013-211}$ ($\times 10^2$)	−5.583(217)		
Coriolis-type interactions					
$(B\zeta^y)^{310-211}$ ($\times 10^2$)	0.18045(986)	$C_{yK}^{310-211}$ ($\times 10^4$)	2.575(203)	$C_{yJ}^{310-211}$ ($\times 10^4$)	−1.3623(971)
$C_{yKK}^{310-211}$ ($\times 10^6$)	−6.829(695)	$C_{yJJ}^{310-211}$ ($\times 10^6$)	0.5348(526)	$C_{xz}^{310-211}$ ($\times 10$)	2.7673(432)
$C_{xzK}^{310-211}$ ($\times 10^3$)	1.2019(302)	$C_{xzJ}^{310-211}$ ($\times 10^3$)	−0.8387(263)	$C_{xzKK}^{310-211}$ ($\times 10^5$)	−0.2354(228)
$C_{xz}^{032-211}$ ($\times 10$)	−0.3733(367)	$C_{xzK}^{032-211}$ ($\times 10^3$)	1.2068(570)	$C_{xzJ}^{032-211}$ ($\times 10^3$)	0.8061(724)
		$C_{xzJK}^{032-211}$ ($\times 10^5$)	−1.846(112)		
$C_{xz}^{230-211}$ ($\times 10$)	0.7757(957)	$C_{xzK}^{230-211}$ ($\times 10^3$)	0.2636(320)	$C_{xzJ}^{230-211}$ ($\times 10^3$)	−0.776(109)

[a] Values in parentheses are the 1σ statistical confidence intervals.
[b] Constrained to the value of resonance interaction parameter obtained on the base of $\Gamma_{D_+ - D_-}$ constant from [2].

We were not able to assign transitions in the recorded spectrum which would belong to the $\nu_1 + \nu_2 + 2\nu_3$, $\nu_2 + 3\nu_3$, $3\nu_2 + 2\nu_3$, and/or $2\nu_1 + 3\nu_2$ bands. At the same time, the presence of strong local perturbations of the "bright" bands $3\nu_1 + \nu_2$ and $2\nu_1 + \nu_2 + \nu_3$ from the "dark" ones $3\nu_2 + 2\nu_3$ and $2\nu_1 + 3\nu_2$ allowed us to fit

the vibrational energies E and rotational parameters A and B of the states (032) and (230), as well. However, one should remember that, (i) (032) and (230) are the "dark" states, (ii) ro-vibrational levels of states (032) and (230) with high J value are involved in the resonance interactions, (iii) the influence of additional vibrational states is neglected in the Hamiltonian used in the fit. As the consequence, the values of parameters E^{230}, A^{230}, B^{230}, E^{032}, A^{032}, and B^{032}, obtained as the results of the fit, should be only considered as the first approximation to the real values.

6. Conclusion

High-resolution Fourier transform spectrum of the H_2S molecule was studied in the region of 8500–8900 cm^{-1}. More than 450 measured transitions yielded 101 and 95 upper ro-vibrational energies of the states (310) and (211), respectively. These energies were fitted using a Watson-type Hamiltonian, A-reduction, I^r representation, taking into account resonance interactions. The derived 28 diagonal and 18 resonance interaction parameters reproduce the ro-vibrational energy levels, used in the fit, with *rms* deviation of 0.0019 cm^{-1}. The intensity totally borrowed effect in the P-branch is experimentally observed and discussed.

Acknowledgments

This work was jointly supported by the National Project for the Development of Key Fundamental Sciences in China, the National Natural Science Foundation of China (20103007, 50121202, and 20210102154), and the Foundation of the Chinese Academy of Science. O. Ulenikov and E. Bekhtereva thank University of Science and Technology of China for guest professorship in the 2004 year.

References

[1] O.N. Ulenikov, A.-W. Liu, E.S. Bekhtereva, O.V. Gromova, L.-Y. Hao, S.-M. Hu, J. Mol. Spectrosc. 226 (2004) 57–70.
[2] A.D. Bykov, O.V. Naumenko, M.A. Smirnov, L.N. Sinitsa, L.R. Brown, J. Crisp, D. Crisp, Can. J. Phys. 72 (1994) 989–1000.
[3] J.K.G. Watson, J. Chem. Phys. 46 (1967) 1935–1949.
[4] J.-M. Flaud, C. Camy-Peyret, J.W.C. Johns, Can. J. Phys. 61 (1983) 1462–1473.
[5] I.N. Kozin, Per Jensen, J. Mol. Spectrosc. 163 (1994) 483–509.
[6] J.-M. Flaud, C. Camy-Peyret, J. Mol. Spectrosc. 55 (1975) 278–310.
[7] O.N. Ulenikov, A.B. Malikova, M. Koivusaari, S. Alanko, R. Anttila, J. Mol. Spectrosc. 176 (1996) 229–235.
[8] O.N. Ulenikov, G.A. Onopenko, M. Koivusaari, S. Alanko, R. Anttila, J. Mol. Spectrosc. 176 (1996) 236–250.